Laser Cladding of Fluorapatite Nanopowders on Ti6Al4V

Amin Nakhi[1], Monireh Ganjali[1,*], Haji Shirinzadeh[2], Ali Sedaghat Ahangari Hossein Zadeh[3], Masoud Mozafari[1]

[1]Nanotechnology and Advanced Materials Department, Materials and Energy Research Center (MERC), P.O. Box 14155-4777, Tehran, Iran
[2]Department of Semiconductors, Materials and Energy Research Center (MERC), P.O. Box 14155-4777, Tehran, Iran
[3]Department of Ceramics, Materials and Energy Research Center (MERC), P.O. Box 14155-4777, Tehran, Iran

*Corresponding author: E-mail: monireh_gan@merc.ac.ir; monireh.gan@gmail.com

In this study, at first fluorapatite nanopowder (nfAp) was initially synthesized by sol-gel method and then deposited on Titanium alloys (Ti-6Al-4V) using laser cladding technique. X-ray diffraction (XRD), Fourier transform infrared spectroscopy (FTIR) and scanning electron microscopy (SEM) equipped with electron dispersive spectroscopy (EDX), were applied to study the crystallite and particle size, phase and chemical structure and microstructure the powder and coating sample. The results of XRD analysis and FTIR showed the presence of fluorapatite phases and ions replacement of F with OH in the structure of apatite. The MTT cell viability assays were used to study the biocompatibility of the coating samples. The average size of the crystallites estimated from XRD patterns using the Scherrer equation was 44 nm. The prepared nfAp coating deposited on Ti6Al4V showed well-behaved biocompatibility properties.

Introduction

Titanium and its alloys such as Ti-6Al-4V are the most common metallic biomaterials that have been of interest in the biomedical applications due to their excellent mechanical and tribological properties. However, despite its desirable properties, the corrosion of Ti6Al4V in physiological environment and the release of Aluminum (Al) and Vanadium (V) in the body cause long-term health problem such as Alzheimer's and neuropathy [1,2]. Therefore, replacing Al and V by some low toxic elements such as Nb, Zr, Pd and Ta [3,4] or surface modification techniques have been proposed to enhance biocompatibility [5,6].

Over the past decades, different physical and chemical methods have been proposed to overcome the above noted drawback and to produce a better biocompatible Ti implant surface. The most common technique is that of the production of apatite layer on them. Among apatite compounds, hydroxyapatite (HAp) is very similar to human hard tissue in morphology and composition [7]. Particularly, it has a hexagonal structure [8,9]. Moreover it can easily form chemical bonds with surrounding tissues [10]. The relative ratio of calcium to phosphorus (Ca/P) is approximately 1.62 which is close to Ca/P ratio in bones [11-13]. Due to some disadvantages such as brittleness, low tensile strength and fracture toughness HAp was not sufficient to be good biomaterials candidate for coating of Ti implant surface. Also, it has been well documented that HAp undergoes phase instability and the decomposition of HAp at high calcination and sintering temperatures [14-16]. Thus,

flourapatite (fAp) because of higher chemical and biocompatibility stability of HAp, corrosion resistance and phase stability at higher temperatures replace to HAp [17,18]. The presence of fluoride ions in fAp increases the absorption of protein and cell adhesion [19]. These factors all occur due to the replacement of the F-ion with OH-ions, which encourages the ion to substitute the process of mineralization and calcium phosphate crystallization in the process of bone formation [20,21].

Sol-gel and plasma spray are two methods that were applied to coat fAp layer on Ti6Al4V surface [22,23]. Although these methods have some advantages, due to mechanical rather than metallurgical bonding between the coating and substrate, there have been few reports concerning the fabrication or characterization of the fAp produced via laser cladding by Chien and colleagues [24]. Laser cladding is an advanced coating technology, which produces extremely dense, crack free and porous microstructure coatings [25]. Moreover, in this method, the bonding between coating layer and substrate is metallurgical and the composition and coating thickness is uniform. In addition, there is heat input to the component and consequently low dilution [26-28].

Most of the research works has been focused on the evaluation of the effect of laser parameters like power and scanning speed on the coating of apatite materials as HAp or fAp powders on Ti6Al4V. However, the biological properties especially MTT analysis of nano fluorapatite (nfAp) powder coating on Ti6Al4V substrate, has not been a concern by most investigators. Therefore, these parameters need further investigation.

Advanced Materials Letters
www.vbripress.com/aml

IAAM®
Advancement of Materials
to Global Excellence
www.iaamonline.com

In the present research, nfAp powder was chosen as a coating material mixed with polyvinyl alcohol (PVA, (C2H4O)n) respectively, and then clad the mixture on Ti-6Al-4V substrates using continuous wave (CW) CO_2 laser beam. A series of experiments are then performed to investigate the effects of the laser processing parameters on the morphology, and the MTT of the various coatings.

Materials and methods

Preparation of nfAp powder

For synthesis of nfAp powder, Triethyl phosphate [TEP, $C_6H_{15}O_4P$; MERK] and ammonium fluoride [NH_4F; MERK] was dissolved in 100ml alcohol and distilled water, and stirred for 24 hours at room temperature. In another container, calcium nitrate tetrahydrate [$Ca(NO3)_2,4H_2O$; MERK] were dissolved in a 100ml distilled water and allowed to stir for 18 hours at room temperature. Then, the solution containing calcium was added drop wise to the solution containing phosphorus and stirred vigorously for 48 hours. The final solution was aged for 24hrs. The prepared gel was dried using a hot air oven (Lenton Furnace, Lenton Thermal Designs Limited, UK) at 80 °C for 72 hours and sintered using conventional pressureless sintering furnace (LT furnace) in air atmosphere at temperature 550 °C for 1h with a ramp of 5 °C/min with 60 hours of dwell time before being cooled down to room temperature. Finally, the prepared fAp was grinded well to a fine powder by using ball milling (Fritsch, Germany). It should be noted that the ratio of the chemical compounds used in calcium to phosphorus and phosphorus to fluorine ratios is 1.67 and 3 respectively [29].

Preparation of substrate

Ti6Al4V plates with dimensions of $30 \times 10 \times 1$ mm were used as substrates in this study. The chemical composition of the Ti6Al4V substrates was determined by optical emission spectrometry (Foundery Master quantometer, Germany). Before coating, the samples were ground with successive SiC papers (400–2000 grit) and polished with a 5 μm diamond paste. The substrates were then treated by sandblast followed by ultrasonic cleaning and then drying.

Preparation of coating materials

Prepared nfAp powder was mixed with PVA by 50:50 in weight % and then well stirred into slurry. The chemical composition of the Ti-6Al-4V alloy used in the present experiments is shown in **Table 1**.

Table 1. Chemical composition (wt-%) of Ti-6Al-4V.

Elements	Al	V	Cu	Mo	Sn	Nb	Pd	Fe	Ti
Atomic %	5.83	3.86	0.15	0.43	0.35	0.35	0.15	0.15	bal

Laser treatment of samples

CW CO_2 laser (λ-10.6 nm, diameter of laser beam – 2mm) with output powers and 48W and scanning speed laser 2 mm/s were used for cladding in this experiment. The laser cladding experiments were conducted in an Ar shielded atmosphere (Ar flow rate: 25 l/min) using a 5° incident angle and a 14 mm defocus length.

Characterization

X-ray diffraction device (XRD-Siemens and Bruker, Erlangen, Germany) (40kV, 30mA) with Cu Kα radiation (λ = 1.54060Å) was used for the structural and the phase analysis of the both synthesized nfAp powder and coating. The functional group of the nfAp powder was identified using the Fourier transform infrared spectroscopy (Perklin elmer Spectrum two) ranging from 400-4000cm^{-1}. The morphology and shape of the synthesized nanopowders and coatings was done by scanning electron microscopy (SEM-XL30; Philips, Eindhoven, The Netherlands) equipped by electron dispersive diffraction (EDX).

MTT test

The viability of nfAp coating on human Caucasian fetal foreskin fibroblast (HFFF 2) was evaluated by MTT [3-(4, 5-dimethylthiazol-2-yl)-2, 5-diphenyltetrazolium bromide] assay. HFFF2 cells were cultured in RPMI1640 (density of about 50000 cells per well) cell media supplemented with fetal bovine serum (Gibco) and penicillin streptomycin. The cells were incubated at 37℃ under an atmosphere of 5% CO2 for 24h. After this, the culture medium was removed and the extract solution of samples with different concentration 25, 50, 75 and 100 % was added to the wells for 24 and 48h. Afterwards the medium and extract was removed and 10 μl MTT solution (5mg/ml) was added to each well Following incubation for 4 h, the liquid was replaced with DMSO (Dimethyle sulfoxide, Sigma) to dissolve the formazan crystals. Afterwards, the plate was placed at 37 °C for 10 min before measurement. The optical density of the cells was measured using micro plate reader (Bio Tek EL × 808). Each experiment was performed in triplicate and the results were reported as mean ± standard deviation. Cell viability was calculated according to formula (2) [30]:

$$V= (Ab/As)\ 100\% \qquad (2)$$

where V is cell viability percentage, Ab is average absorbance of the test sample, and As is mean absorbance of the control.

Results and discussion

The XRD, FTIR, SEM and EDX analysis of nfAp powder are shows in **Fig. 1 a-d**. A diffraction patterns of nfAp powder according to standard (JCPDS#15–0876) in the range of $2\theta = 20–60$ are shown in **Fig. 1a**. The crystalline size was calculated by using the debye scherrer formula [31]. The average crystalline size of the synthesized fAp powder is 44nm. In the figure 1, the peaks of this sample are in good agreement with the fluorine apatite phase. Also it can be assumed that the peaks shifted to higher positions (2θ) relative to the hydroxyapatite phase by fluorine-hydroxyl exchange in apatite. Due to the smaller ionic radius of ion-fluorine compared to hydroxyl groups

Advanced Materials Letters
www.vbripress.com/aml

IAAM®
Advancement of Materials
to Global Excellence
www.iaamonline.com

[32], this substitution causes a structural distortion (interplanar spacing decreases). In this case, the interplanar spacing (d) decreases, so according to the Bragg's law (2d sinθ=nλ), the scattering angle (θ) increases, because the wavelength of the incident wave is constant. It means that as a substitution causes the peaks shifted to higher positions (2θ). Wei *et al.,* [33] showed that fAp peaks are sharper than hydroxyapatite (HAp), which can be due to the presence of fluorine ion in the structure. This presence greatly increases the crystallinity, which leads to a decrease in the solubility of fluorapatite phase.
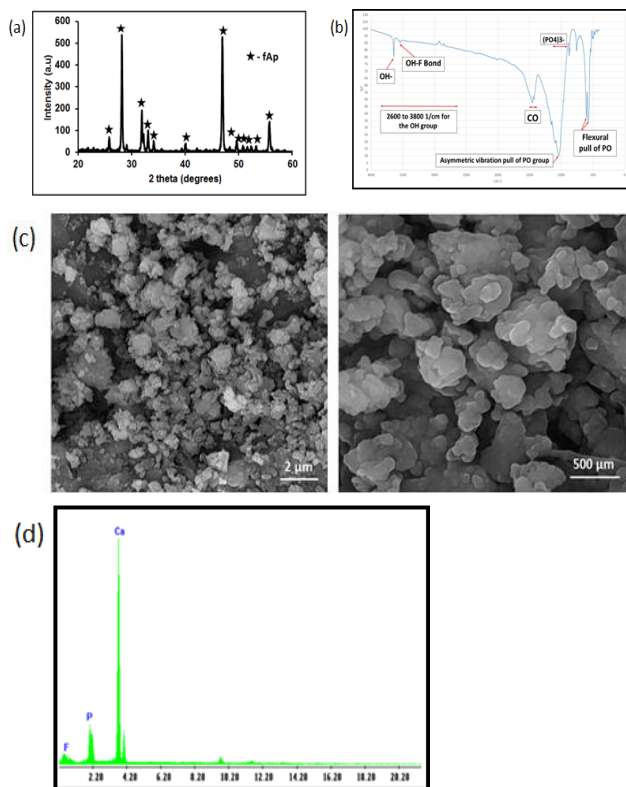

Fig. 1. (a) XRD patterns of fAp powder,(b) FTIR of fAp powder; (c) and (d) SEM images and EDX analysis of the nfAp powder.

The bands or functional group of the nfAp powder shows in **Fig. 1b**. The FTIR spectrums of fAp powder in 576.33 and 602.31 cm^{-1} show the flexural pull of PO and at 301.040 cm^{-1} shows the asymmetric vibration of the PO group. The wide peak of 2600 to 3800 cm^{-1} is related to the OH group. The small peaks between 3536 cm^{-1} and 3545 cm^{-1} correspond to the OH -F bond, which indicates the penetration of phosphate ion into the apatite network. Suchanek *et al.,* [34] showed an OH-vibrational state of about 630 cm^{-1}, which is shown in **Fig. 2**. The peak in the region of 3643.25 cm^{-1} is related to the hydroxyl group, which is the hydroxyl group formed by the hydrogen bonding of fluoride ions. This peak verifies the structure of crystalline fAp with the hydroxyl group. These observations for fAp powder are due to hydrogen, and the formation of the bond between F and OH represents the replacement of F ions with OH ions in the structure of

apatite. Substitution of different ions in the apatite structure reduces the symmetry in the FTIR spectrum. The presence of a wide and sharp peak in the range of 900-1100 cm^{-1} represents the group $(PO_4)^{3-}$ [35]. The stretching and bending modes for $(PO4)^{3-}$ are shown in both 575.70 and 602.31 cm^{-1}. The band 956 cm^{-1} is for the group $(PO4)^{3-}$ with fluorhydroxyapatite (fHAP) and fAp. The range of 963 cm^{-1} and 1500-1400 cm^{-1} is related to the CO group, which is related to carbonate ion of the hydroxide apatite powder.

Figs 1c-d shows SEM images for different magnifications (10,000X and 50,000X) and EDX of the nfAp powder. The morphology of nfAp powder is spherical and homogenous as confirmed by Montazeri *et al.,* [36]. The average size of particles was measured by ImageJ software, which was about 85 nm, which is a similar result to other researchers. [37,38].

XRD spectrum of the coated sample shows in Fig. 4. The predominant peaks in the patterns of the coating layer of the samples is mainly composed of fAp, CaTiO2, Al2O3 and Ca3(PO4)2 phases. fAp has a hexagonal structure with the lattice constants of 0.9423 nm and c of 0.6875 nm. It seems that $CaTiO_2$ was combined from fAp and Ti-6Al-4V, and $Ca_3(PO_4)_2$ was decomposed from fAp at a temperature higher than 1057°C [39]. It indicates that fAp coating can be synthesized by laser cladding.

SEM images of cross-section of nfAp powder on Ti6Al4V shows in **Fig. 2b**. As can see form this figure, the bonding between the coatings layer and substrate is well. The perpendicular crack from coating to substrate was observed due to using PVA as a binder [40].
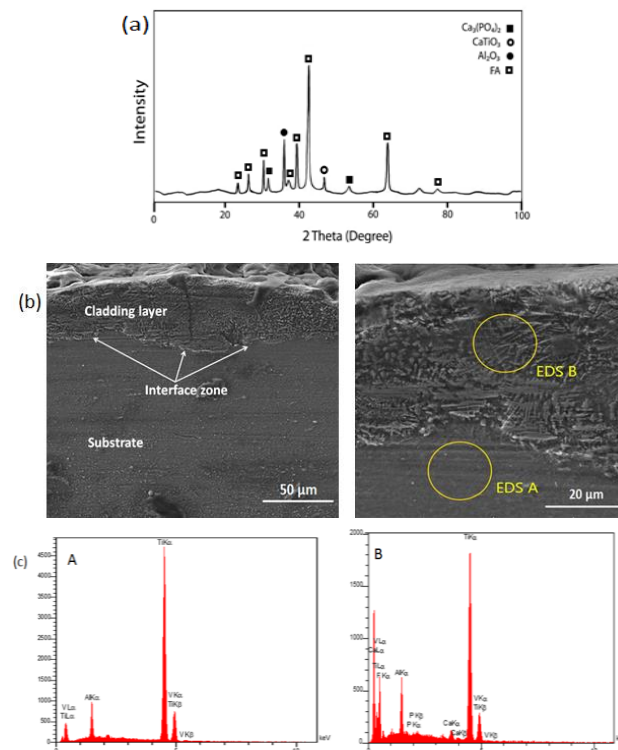

Fig. 2. (a) XRD, (b) SEM and (c) EDX analysis of coated sample.

Advanced Materials Letters
www.vbripress.com/aml

IAAM®
Advancement of Materials
to Global Excellence
www.iaamonline.com

It can also be seen that the cladded layer is mixed with the substrate and metal-ceramic layer on the surface is created [41]. Microstructure of the cross-section of coated layer consists cellular dendritic crystal, which grows along the direction of heat flow by the temperature gradient. The EDX analysis, **Fig. 2c** also indicates the presents of fluorapatite in the coated layer. According to the EDX result, Al and V elements can be seen in the coated layer because partial Al and V element are diffused from the substrate into the coating.

The cell viability of cell cultures treated with the suspensions of the nfAp coating in the different concentration from 25 to 100% and the duration time from 24 to 48 h are given in **Fig. 3**. As shown in **Fig. 3**, the increase in the concentration and duration times, the cytoxity is decreased. Since the criterion of non-toxicity is the percentage of cellular survival above 70%, according to the **Fig. 3**, none of the concentrations investigated in the two studied periods have been shown to have toxicities [42].
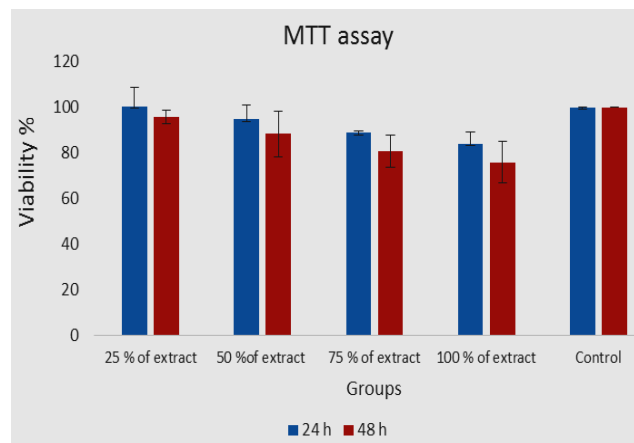

Fig. 3. Cytotoxicity analysis of nfAp coating of HFF-2 cell lines after 24 and 48. Each bar represents the mean of three measurements ± SD.

Conclusion

In this study nfAp powder was coated on TI6Al4V substrates by laser cladding method. The XRD and FTIR results of nfAp powder showed the replacement of F-ion with OH-and the formation of fAp phase. Moreover, according to XRD patterns different phases like fAp, $CaTiO_2$, Al_2O_3 and $Ca_3(PO_4)_2$ were formed on the coating layer. Based on SEM microstructural analysis it can be concluded that homogeneous, crack free and well bonding coating can be obtain using laser cladding method. In addition, the cytotoxic tests showed the coated samples have good biocompatibility and the sample coated from the solution with 25% of extract solution has the best biocompatibility.

References

1. Geetha, M.; Singh, A.K.; Asokamani, R.; Gogia, A.K.; *Progress in Materials Science*, **2009**, *54,* 397.
2. Navarro, M.; *Journal of The Royal Society Interface,* **2008**, 5, 1137.
3. Elschner, C.; Noack, C.; Preissler, C.; Krause, A.; Scheler, U.; Hempel, U.; *J. Mater. Sci. Technol.,* **2015**, *31,* 427.
4. Fellah, M.; Labaïz, M.; Assala, O.; Dekhil, L.; Iost, A.; *Matériaux Tech.,* **2014**, *102,* 606.
5. Chien, C.S.; Kuo, T.Y.; Liu, C.W.; Lin, H.C.; Liao, T.Y.; Hong, T.F.; Lee, T.M.; *Material Research Innovations*, **2015**, *19,* S5-1318.
6. Rasmi, R.; Abshar, H.; Mamilla, R.; Lalit, M.; *Surface and Coatings Technology,* **2018**, *352,* 420.
7. Wei, G.; Ma, P.X.; *Biomaterials,* **2004**, *25,* 4749.
8. Kalita, S.J.; Bhardwaj, A.; Bhatt, H.A.; *Materials Science and Engineering*: C, **2007**, *27,* 441.
9. Mostafa, N.Y.; Brown, P.W.; *Journal of Physics and Chemistry of Solids,* **2007**, *68,* 431.
10. Chien, C.S.; Ko, Y.S.; Kuo, T.Y.; *J. Med. Biol. Eng.,* **2015**, *35,* 357.
11. Teixeira, S.; Rodriguez, M.A.; Pena, P.; De Aza, A.H.; De Aza, S.; Ferraz, M.P.; Monteiro, F.J.; *Materials Science and Engineering: C,* **2009**, *29,* 1510.
12. Guo, L.; Huang, M.; Zhang, X.; *Journal of Materials Science: Materials in Medicine,* **2003**, *14,* 817.
13. Nasser, Y.M.; *Mater Chem Phys.,* **2005**, *94,* 333.
14. Nilen, R.W.; Richter, P.W.; *J. Mater Sci Mater Med.*, **2008**, 19, 1693.
15. Muralithran, G.; Ramesh, S.; *Ceram Int.,* **2000**, *26,* 221.
16. Pattanayak, D.K.; Dash, R.; Prasad, R.C.; Rao, B.T.; Rama Mohan, T.R.; *Science and Engineering: C*, **2007**, *27,* 684.
17. Chien, C.S.; Ko, Y.S.; Kuo, T.Y.; *J. Med. Biol. Eng.,* **2015**, *35,* 357.
18. Chien, C.S.; Liao, T.Y.; Hong, T.F.; *Surface & Coatings Technology,* **2011**, *205,* 3141.
19. Fathi, MH.; Mohammadi Zahrani, E.; Zomorodian, A.; *Materials Letters,* **2009**, *63,* 1195.
20. Legeros, R.Z.; Silverstone, L.M.; Daculsi, G.; Kerebel, L.M.; *J. Dent. Res.,* **1985**, *62,* 138.
21. Aoba, T.; *Crit Rev Oral Biol,* **1997**, *8,* 136.
22. Tredwin, C.J.; Young, A.M.; Georgiou, G.; Shin, S.H.; Kim, H.W.; Knowles, J.C.; *Dental Materials,* **2013**, *29,* 166.
23. Kangasniemi, I.M.; Verheyen, C.C.; Van der Velde, E.A.; Groot, K.; *J. Biomed Mater. Res.,* **1994**, *28,* 563.
24. Chien, C.S.; Liao, T.Y.; Hong, T.F.; Kuo, T.Y.; Chang, C.H.; Yeh, M.L.; Lee, T.M.; *Journal of Medical and Biological Engineering,* **2014**, *34,* 109.
25. Mohammadzadeh Asl, S.; Ganjali, M.; Karimi, M.; *Surface and Coatings Technology,* **2019**, *363,* 236.
26. Quintino, L.; Chapter 1: Overview of coating technologies, in book: Surface Modification by Solid State Processing, **2014**, Pages 1-24, Woodhead Publishing.
27. Toyserkani, E.; Khajepour, A.; Corbin, S.; Laser Cladding, CRC Press, **2005**, 260
28. Ready J.F.; (Ed.), LIA Handbook of Laser Materials Processing, Chapter 8: Surface Treatment: Glazing, Remelting, Alloying, Cladding, and Cleaning, Laser Institute of America, **2001**, p. 263-297.
29. Chien, C.S.; Ko, Y.S.; Kuo, T.Y; Liao, T.Y.; Hong, T.F.; Lee, T.M.; *Advanced Materials Research,* **2011**, *287,* 2225.
30. Nassar, E.J.; Ciuffi, K.J.; Calefi, P.S.; Rocha, L.A.; De Faria, E.H.; MLA. e Silva, Luz, P.P.; Bandeira, L.C.; Cestari, A.; Fernandes, C.N.; Chapter 1: Biomaterials and Sol-Gel Process: A Methodology for the Preparation of Functional Materials. In Biomaterial, Science

and Engineering, 1st Ed.; R. Pignatello, Ed.; InTech open, **2011**, p. 3–30.

31. Sasani, N.; Khadivi Alaska, H.; Zebarjad, S. M.; Vahdati Khaki, J.; *Journal of Ultrafine Grained and Nanostructured Materials,* **2013**, *46,* 31.
32. Cullity B.D.; Elements of X-ray Diffraction. 2nd ed. Morris Cohen, Editor. Reading, MA: Addison-Wesley Publishing; **1977**.
33. Rodrıguez-Lorenzo, L.M.; Hart, J.N.; Gross, K.A.; **2003**, *24,* 3777.
34. Wei, M.; Evans, J.H.; Bostrom, T.; Grøndahl, L.; *Journal of Materials Science: Materials in Medicine,* **2003**, *14,* 311.
35. Suchanek, W.; Yoshimura, M.; *J. Mater. Res.,* **1998**, 13, 94.
36. Cavalli, M.; Gnappi, G.; Montenero, A.; Bersani, D.; Lottici, P.P.; Kaciulis, S.; Mattogno, G.; Fini, M.; *Journal of Materials Science,* **2001**, *36,* 3253.
37. Montazeri, N.; Jahandideh, R.; Biazar, E.; *Int. J. Nanomedicine,* **2011**, *6,* 197.
38. Karimi, M.; Ramsheh, M.R.; Ahmadi, S.M.; Madani, M.R.; Shamsi, M.; Reshadi, R.; Lotfi, F.; *Materials Science & Engineering C,* **2017**, *1,* 121.
39. Chien, C.S.; Liu C.W.; Kuo, T.Y.; *Materials,* **2016**, *9,* 380.
40. Chien, C. S.; Han, T. J.; Hong, T. F.; Kuo T. Y.; Liao, T. Y.; *Materials Transactions,* **2009**, *50,* 2852.
41. Tlotleng, M.; Akinlabi, E.; Shukla, M.; Pityana, S.; *Materials Science and Engineering: C,* **2014**, *43,* 189.
42. Forghani, A.; Mapar, M.; Kharaziha, M.; Fathi, M. H.; Fesharak, M.; *Int. J. Appl. Ceram. Technol.,* **2012**, 1.